Received: 24 March 2021 | Revised: 18 June 2021 | Accepted: 18 June 2021

DOI: 10.1096/fba.2021-00039

REPRODUCIBILITY REPORT

FASEB BioAdvances WILEY

OX40-targeted immune agonist antibodies induce potent antitumor immune responses without inducing liver damage in mice

Yee C. Tee[1,2] | Stephen J. Blake[1] | David J. Lynn[1,2]

[1]Precision Medicine Theme, South Australian Health and Medical Research Institute, Adelaide, SA, Australia

[2]Flinders Health and Medical Research Institute, Flinders University, Bedford Park, SA, Australia

Correspondence
David J. Lynn, Precision Medicine Theme, South Australian Health and Medical Research Institute, Adelaide, SA, Australia.
Email: David.Lynn@sahmri.com

Funding information
This work was supported by an Ideas Grant (APP1190799) from the Australian National Health and Medical Research Council (NHMRC) awarded to S.J.B. and D.J.L. The contents of the published material are solely the responsibility of the authors. This work was also supported by an EMBL Australia Group Leader award to D.J.L.; a Tour De Cure Pioneering Research Grant (RSP-264-18/19); and a Flinders Foundation Health Seed Research Grant.

Abstract

Despite promising preclinical and clinical data demonstrating that immune agonist antibody immunotherapies (IAAs) such as αOX40 induce strong antitumor immune responses, clinical translation has been significantly hampered by the propensity of some IAAs to induce dose-limiting and sometimes life-threatening immunotoxicities such as cytokine release syndrome and hepatotoxicity. For example, in a recent study αOX40 was shown to induce significant liver damage in mice by inducing the pyroptosis of liver natural killer T cells (NKT) cells. Surprisingly; however, given these previous reports, αOX40 treatment in our hands did not induce NKT cell pyroptosis or liver damage. We investigated numerous potential confounding factors including age, sex, tumor burden, dosing strategy, and the gut microbiota, which could have explained this discrepancy with the previous study. In none of these experiments did we find that αOX40 induced any more than very mild inflammation in the liver. Our study therefore suggests that, preclinically, αOX40 is a safe and effective immunotherapy and further studies into the clinical benefit of αOX40 are warranted.

KEYWORDS

hepatoxicity, immune agonist antibody, immunotherapy, liver, microbiota, natural killer T cells, OX40, tumor

1 | INTRODUCTION

Immune checkpoint inhibitors (ICIs) targeting T-cell inhibitory molecules can induce long-term, potentially curative clinical responses in some cancers that are unresponsive to conventional therapy.[1] The efficacy of ICI therapy is, however, restricted to a relatively small number of cancer types; most notably melanoma and non-small-cell lung cancer, both solid tumors with heavy mutational burdens and high levels of immune cell infiltrate.[2,3] Tumors with poor immune cell infiltratation, due to

Abbreviations: ABX, antibiotic exposed; ALT, alanine aminotransferase; ConA, Concanavalin A; gMFI, geometric mean fluorescent intensity; IAA, immune agonist antibodies; ICI, immune checkpoint inhibitors; irAE, immune-related adverse event; NKT, natural killer T cell; SOPF, specific and opportunistic pathogen free.

Stephen J. Blake and David J. Lynn joint senior authors.

low mutational burden or development in immune privileged sites, otherwise known as “cold” tumors, uniformly respond poorly to ICIs.[4] Thus, there is a unmet need for treatments that can drive immune cell infiltration into “cold” tumors to sensitize them to ICI therapies. One such strategy that is being assessed is to combine immune agonist antibodies (IAA) with ICIs to enhance their response in “cold” tumors.

IAAs target co-stimulatory molecules on immune cells, enhancing multiple downstream processes ranging from increased proliferation and cytokine production to resistance to apoptosis.[5] IAAs can increase the infiltration of immune cells into the tumor microenvironment, activating direct antitumor responses and increasing tumor sensitivty to ICIs.[6,7] However, despite numerous examples of IAAs inducing a beneficial antitumor effect in both clinical and preclinical settings,[8,9] the development of IAAs has been hampered by their propensity to induce high-grade and sometimes fatal immune-related adverse events (irAEs). IAAs targeting OX40 (αOX40) are promising cancer immunotherapies that are being assessed in preclinical studies and ongoing phase I–II clinical trials.[10] Encouragingly, αOX40 treatment has been shown to increase tumor-infiltrating lymphocytes and to induce a proinflammatory tumor microenvironment (TME) in both mice and humans, suggesting that αOX40 could be a promising therapy to use in combination with ICIs.[6,7,11] A potential concern, however, is that αOX40 has been shown to induce significant liver damage in preclinical models through a natural killer T (NKT) cell-dependent pathway.[12] More specifically, Lan et al.[12] found that OX40 was highly expressed on NKT cells and that treatment with αOX40 induced pyroptosis of liver NKT cells resulting in significant liver necrosis and damage. Reports of such significant toxicity in preclinical models could dampen enthusiasm for the clinical translation of αOX40 immunotherapies.

Here, we report that despite extensive testing of the same αOX40 antibody as used by Lan et al., using different dosing strategies, in a range of different experiments using tumor-bearing and tumor-free mice of different ages and sex, we did not find that αOX40 induced significant liver toxicity or cytokine release syndrome (CRS) as has been previously reported. Given these data, we conclude that αOX40 does not induce significant liver damage or cytokine release syndrome in mice, suggesting that αOX40 is a promising immunotherapy with a good safety profile in preclinical models and therefore should be further assessed for evidence of antitumor efficacy in combination with ICI immunotherapies.

2 | MATERIAL AND METHODS

2.1 | Mice

All mice were maintained in a PC2, specific and opportunistic pathogen-free (SOPF) animal facility located at the South Australian Health and Medical Institute (SAHMRI). Three- to nine-week-old male and female C57BL/6 mice were used in experiments as indicated in the figure legends. Mice were bred and maintained at the SAHMRI Bioresources facility, with colony founder mice purchased from the Jackson Laboratories. Experiments were all approved prior to commencement by the SAHMRI animal ethics committee. Researchers were not blinded to the treatment groups.

2.2 | MC38 tumor cell culture, inoculation, and monitoring

MC38 cells were kindly donated by Dr Susan Woods from SAHMRI. Cells were confirmed negative for mycoplasma contamination by routine testing with the MycoAlert™ Mycoplasma Detection Kit (LT07-418, Lonza, BSL, CH). Cryopreserved MC38 tumor cells were thawed and cultured in a T75 flask (156499, Thermo-Fisher) with Dulbecco's Modified Eagle Medium (DMEM, 11960-044, Gibco) and supplemented with penicillin–streptomycin (P4333-100ML, Sigma-Aldrich), 2 mM glutamine (35050038, Gibco), 1 mM sodium pyruvate (11360070, Gibco) and 10% foetal bovine serum (FBS, ASFBS-U, Assay Matrix), and cultured at 37°C in 10% CO_2. Cells were subcultured three times weekly, with trypsin-EDTA (T4049-500ML, Sigma-Aldrich) used to detach confluent cells. For tumor inoculation, single-cell suspensions were generated from log-phase cells of 60%–80% confluency that were counted and resuspended in DMEM with no additives and 100 μl (1×10^6) of MC38 cells were injected subcutaneously into the right flank of mice. Tumors were monitored and measured regularly by Vernier calipers. Tumor size was calcuated as mm^2 by determining the width and length of the tumor.

2.3 | Immunotherapy

Mice were intraperitoneally (i.p.) injected with αOX40 clone OX-86 (BE0031, BioXCell) at the timepoints and dosages indicated in the figure legends. Control mice were injected with an equivalent volume of phosphate-buffered saline (PBS, D8537-500ML, Sigma-Aldrich).

2.4 | Flow cytometry

Livers were dissected from mice and crushed between two frosted glass slides in RPMI 1640 (R8758-500ML, Sigma-Aldrich) with 1% FBS and passed through a 70-μm cell strainer to generate a single-cell suspension. Suspensions were washed in RPMI 1640 (R8758, Sigma-Aldrich) and 1% FBS and centrifuged at 350 × g for 5 min. Leukocytes were isolated via single layer 37.5% Percoll density gradient (P1644, GE healthcare), centrifuged at 690 × g for 12 min at 15°C. Cells were then resuspended in ammonium-chloride-potassium lysis buffer (555899, Becton Dickenson) and incubated at room temperature for 2 min to lyse red blood cells and then washed twice in FACS buffer (PBS, 0.1% bovine serum albumin (BSA, SBSA, AusGeneX), 2 μM EDTA (15575020, Gibco)) before use. MC38 tumors were dissected from the flank of mice and cut into ~1–4 mm^3 pieces and digested with the following digestion buffer: RPMI 1640, 1% FCS, 1 mg/ml Collagenase D (17104019, Thermofisher) and 100 μg/ml DNAse I (47167288001, Roche) for 1 hr at 37°C. Digested tumors were then passed through a 40-μm cell strainer to obtain a single-cell suspension before being washed once with RPMI and 1% FCS and resuspended in FACS buffer for use.

Both liver and tumor immune cells were incubated with FC Block (553141, BD Biosciences) and then stained with the following antibody panels. To quantify NKT and T-cell populations in livers or tumors, cells were stained with TCRβ-FITC (553171, BD Biosciences), NK1.1-APC (130-112-237, Miltenyi), CD11b-BV711 (563168, BD Biosciences), CD4-BV510 (563108, BD Biosciences), CD8-BUV395 (563786, BD Biosciences), Ly6G-PEcy7 (560601 BD Biosciences), and CD1d Tet-PE (kindly provided by NIH tetramer facility) on ice for 40 min. Cells per gram of organ were enumerated by the addition of Liquid Counting Beads (335925, Becton Dickenson) which were used to determine cells per sample following instructions provided by the manufacturer. Dead cells were excluded from analysis by adding DAPI (564907, BD Biosciences) directly before running. The gating strategy to assess liver (Figure S1) and tumor (Figure S2) immune cell populations is shown in the supplementary data. To evaluate the expression of OX40 on cell subsets, the same antibody panel described above was used with the addition of OX40-BV421 (740061, BD Biosciences). To identify Treg cells, Zombie Aqua fixable dye (423101, Biolegend) was used instead of DAPI to exclude dead cells and cells were surface stained with TCRβ-FITC, CD4-PEcy7 (100528, BD Biosciences), and CD8-APCcy7 (557654, BD Biosciences). Subsequently, cells were fixed and permeabilized with Intracellular Fixation & Permeabilization Buffer (88-8824-00, eBiosciences) before being stained for FoxP3-Alexa647 (560401, BD Biosciences) for 30 min on ice. The gating strategy to identify Treg cells is shown in (Figure S3). All flow cytometry was done on a Fortessa X-20 flow cytometer (Becton Dickenson) and analyzed with Flowjo 10.6.2 (Treeestar, Inc.).

2.5 | Cytokine analysis

Blood from mice was collected by tail bleeding and centrifuged to collect serum. The LEGENDplex™ Mix and Match cytometric bead array (CBA, BioLegend) system was then used to assess the serum concentrations of TGF-β, TNF-α, IL-1β, IL-18, and IL-6 and was analyzed using a Fortessa X-20 (BD Biosciences) cytometer as per the manufacturer's instructions.

2.6 | Alanine amino transferase assay

Alanine amino transferase (ALT) was measured in serum using a Liquid ALT (SGPT) Reagent Set (Pointe Scientific). The manufacturer's instructions were followed except that the reaction volume was scaled down so that a 96-well plate could be used. A quantity of 5 μl of serum was diluted 1:4 with PBS and plated onto black-sided, clear bottom 96-well plates (Corning) and warmed to 37°C. Samples were then mixed with ALT reagent and repeat measurements at 340 nm absorbance were taken every minute over a 5-minute period using a Synergy™ HTX Multi-mode plate reader. ALT activity (international units/L (IU/L)) was then calculated using the equation provided by the manufacturer. Blank wells containing PBS were used to measure background which was then subtracted from sample values to derive the final ALT levels.

2.7 | Histological analysis of livers

Sections of liver were fixed in 10% neutral-buffered formalin for 7 days and then transferred into 80% ethanol for long-term storage. Liver sections were then cut with a microtome, embedded in paraffin, and stained with hematoxylin and eosin (H&E). Liver embedding in paraffin and H&E staining was carried out by the University of Adelaide Health and Medical School's Histology Department. Images of H&E-stained slides were acquired by the SAHMRI histology screening service on a SCN400 F Brightfield and Fluorescence Slide Scanner (Leica Microsystems) at 20 × magnification. CaseViewer (3DHISTECH Ltd) was then used to visually score regions of inflammation based on the following criteria set by Mayer et al.[13] while blinded to treatment groups:

1. Portal inflammation: 0, no inflammatory infiltrate; 1, low level of inflammatory cell infiltration; 2, moderate level of inflammatory cell infiltration; 3, severe inflammation.
2. Lobular inflammation: 0, no inflammatory infiltrate; 1, low level of inflammatory cell infiltration; 2, moderate level of inflammatory cell infiltration; 3, severe inflammation (>50% of parenchyma).
3. Necrosis: 0, none; 1, small necroses; 2, large necrotic areas; 3, bridging necroses.

2.8 | Antibiotic treatment

Antibiotic-exposed (ABX) mice were given 0.5 mg/ml neomycin (N1876, Sigma-Aldrich) and 1 mg/ml ampicillin

(A0166 Sigma-Aldrich) via their drinking water. Mice had access to antibiotic-treated water *ad libitum* for the duration of the experiment and antibiotic supplemented water was changed three times each week. Depletion of gut bacteria was confirmed via 16S rRNA gene RT-qPCR of fecal samples (see Section 2.10). Untreated (No ABX) mice had access to untreated sterilized water *ad libitum*.

2.9 | Fecal DNA extractions

Fecal samples from mice were collected at the indicated timepoints and frozen at −80°C until used. Fecal samples were then thawed, weighed, and broken up in 1 ml of PBS. The fecal suspension was then centrifuged at 10,000 × g for 10 min at 4°C. Supernatant was discarded and the DNA from the pellet was extracted using the Qiagen DNeasy PowerLyzer PowerSoil Kit (12855-100, Qiagen) following the manufacturer's instructions. Briefly, the pellet was resuspended in PowerBead solution and then homogenized to lyse cells using the 2 × 60 second pulse on 6.5 m/s setting on a Persellys FastPrep-24™ (MP Biomedicals). Homogenized samples then underwent a series of washes to remove non-DNA material. DNA was then collected in spin column filters and eluted with RNAse- and DNAse-free water (UPW-100, Fischer Biotec). DNA was then stored at −80°C until further use.

2.10 | 16S rRNA gene real-time quantitative polymerase chain reaction

Real-time quantitative polymerase chain reaction (RT-qPCR) with primers targeting the 16S rRNA gene in bacteria was performed to quantitatively assess bacterial load in ABX and untreated mice. RT-qPCR was performed on DNA extracted from feces at the indicated timepoints and samples compared to a known serially diluted 16S rRNA gene standard derived from *E. coli* according to Nadkarni et al.[14] to estimate the bacterial equivalents in the fecal sample. RT-qPCR was performed on a Quant Studio 7 Flex Real-time PCR system (Thermofisher) on 384-well plates (4343814, Life Technologies) using the SYBR™ Green PCR Master Mix (4309155, Life Technologies) with the primers: 16S-qPCR forward: TCCTACGGGAGGCAGCAGT and 16S-qPCR reverse: GGACTACCAGGGTATCTAATCCTGTT. Primers were purchased from Sigma-Aldrich.

2.11 | Concanavalin A administration

Eight-week-old male C57BL/6 mice were intravenously injected through the tail vein with 15 mg/kg of 0.22-μM filter-sterilized Concanavalin A (ConA) (L7647-25MG, Sigma-Aldrich) in PBS. Serum and tissue were collected 8 hr post-treatment. Control mice were injected with an equivalent volume of PBS.

2.12 | Statistical analysis

All statistical analysis was done using GraphPad Prism 8 (version 8.4.3, GraphPad Software Inc.). For pairwise comparisons statistical significance was assessed via a Mann–Whitney test. For multiple group comparisons, a two-way ANOVA with Bonferroni correction was used. $p \leq 0.05$ was considered statistically significant.

3 | RESULTS

3.1 | A single high-dose αOX40 treatment does not induce hepatotoxicity

As αOX40 is currently being investigated as an immunotherapy in several clinical trials, we were interested in evaluating the toxicity of αOX40 in tumor-bearing mice. Using the same dosing strategy as Lan et al.,[12] we treated MC38 tumor-bearing mice with a single 200 μg dose of αOX40 (Figure 1A). We found that αOX40 induced a notable but not statistically significant decrease in tumor burden in these mice compared to control ($p = 0.0952$ at day 16 using the Mann–Whitney test, Figure 1B). Additionally, we also observed that αOX40 significantly reduced the proportion of tumor-infiltrating Treg cells (Figure 1C), which has also been observed in other studies.[15] Interestingly, given previous reports of αOX40-induced hepatotoxicity,[12] serum ALT levels were not significantly increased in mice treated with

FIGURE 1 Single high-dose αOX40 treatment does not induce hepatotoxicity. (A) Overview of experimental design. (B) MC38 tumor growth after administration of αOX40 (200μg; once) or control (PBS) was assessed by caliper square measurements. (C) Proportion of tumor-infiltrating TCRβ$^+$CD4$^+$Foxp3$^+$ regulatory T cells (Treg cells). (D) Serum ALT levels assessed 14 days after control or αOX40 treatment. (E) Representative H&E-stained sections of liver tissue and (F) total liver histological score, (G) portal inflammation score, (H) lobular inflammation score, and (I) necrosis score. Scale bars are 200μm in length. Total histological score (F) is the sum of (G–I). (J) Representative flow cytometry gates assessing liver natural killer T cells (NKT; CD1d-tetramer$^+$TCRβ$^+$) and (K) number of NKT cells per gram of liver. A Mann–Whitney test was used to assess statistical significance. Data are shown as mean ± SEM (n=5/group). *$p \leq 0.05$; n.s. not significant

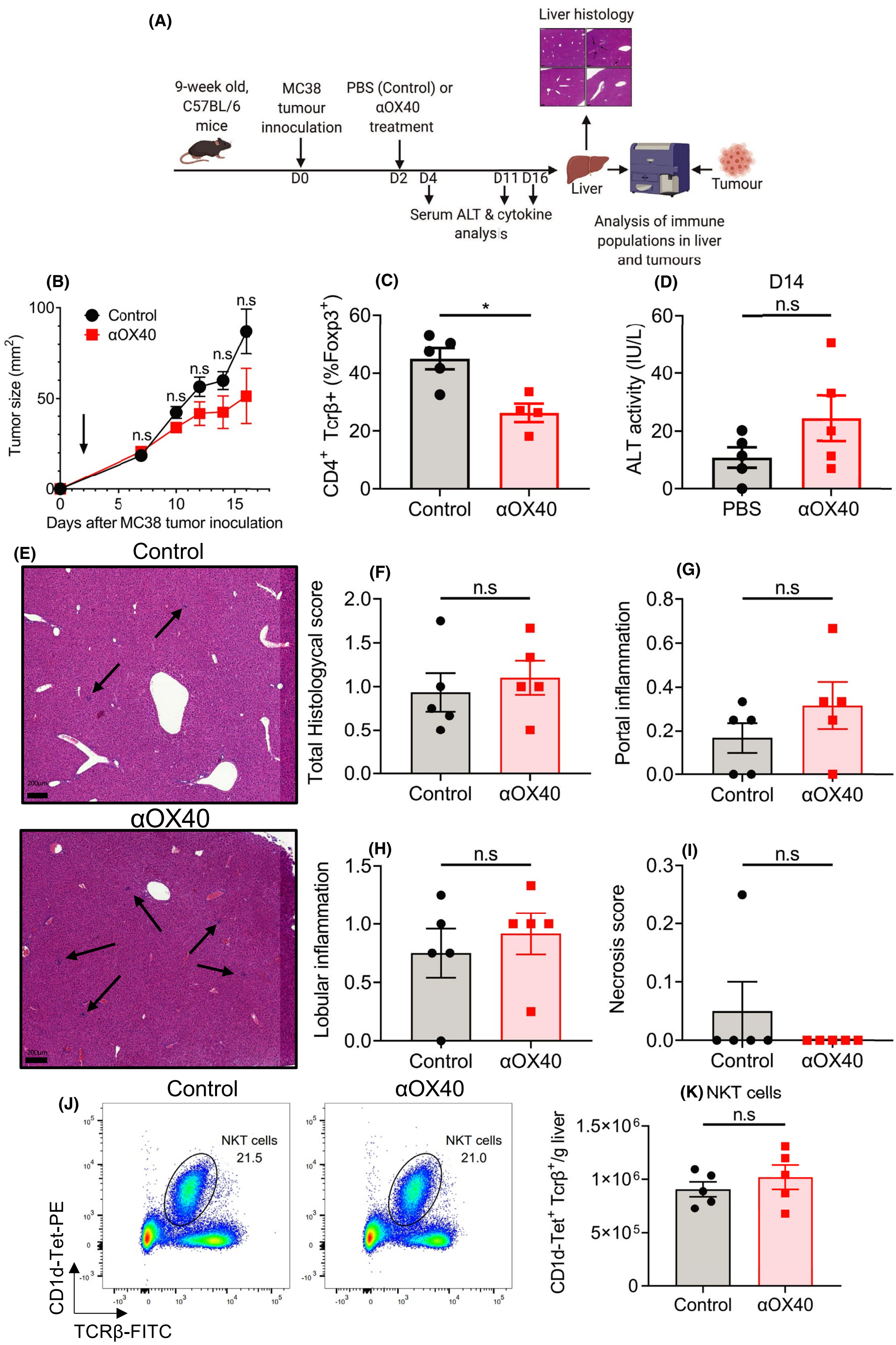
(A)
Liver histology
9-week old, C57BL/6 mice
MC38 tumour innoculation
PBS (Control) or αOX40 treatment
D0
D2 D4
D11 D16
Liver
Tumour
Serum ALT & cytokine analysis
Analysis of immune populations in liver and tumours
(B)
Control
αOX40
n.s
Tumor size (mm²)
Days after MC38 tumor inoculation
(C)
CD4+ Tcrβ+ (%Foxp3+)
*
Control
αOX40
(D)
D14
n.s
ALT activity (IU/L)
PBS
αOX40
(E)
Control
αOX40
(F)
n.s
Total Histologycal score
(G)
Portal inflammation
(H)
Lobular inflammation
(I)
Necrosis score
(J)
Control
αOX40
NKT cells
21.5
21.0
CD1d-Tet-PE
TCRβ-FITC
(K) NKT cells
CD1d-Tet+ Tcrβ+/g liver

αOX40 (Figure 1D). Consistent with these data, histological analysis of H&E-stained sections of liver also revealed no significant differences in histological score between control and αOX40-treated mice (Figure 1E–I). Prior reports have indicated that αOX40 induces significant liver necrosis by inducing pyroptosis of liver NKT cells. Consistent with the lack of liver damage observed in our experiments, flow cytometry analysis showed that liver NKT cells were not depleted in αOX40-treated mice (Figure 1J–K). We investigated whether higher doses of αOX40 (300–500 μg) would induce liver damage in mice. However, at all doses tested, we did not observe αOX40 to cause either a significant loss of NKT cells or significantly increased serum ALT (Figure S4A–C). Taken together, our data suggest that, using the same (or higher) dosing strategy as Lan et al.,[12] αOX40 does not induce significant hepatotoxicity in mice, in contrast to these previous reports. αOX40 did induce changes in the TME and in tumor growth suggesting that the antibody used was functionally competent.

3.2 | The gut microbiota plays a role in mediating immune responses to αOX40 treatment in the liver

We next considered potential reasons for the different results observed by us and Lan et al. Previous studies of other IAAs such as αCD40 and αCD137 have reported that repeated administration of these IAAs at a lower dose induces hepatotoxicity similar to the hepatotoxicity shown by Lan et al., albeit driven by other types of immune cells.[16-18] We therefore investigated whether a repeated dosing strategy (100 μg of αOX40 administered three times, 4 days apart) was required for αOX40 to induce liver damage. Additionally, we considered that differences in the gut microbiota of mice in our study and in the Lan et al. study could potentially explain our discordant results, since previous studies have demonstrated that the gut microbiota has strong immunomodulatory effects on the activity of liver NKT cells,[19,20] which Lan et al. showed were required for αOX40-induced hepatotoxicity in their study.[12] To evaluate if the gut microbiome influences the toxicity of αOX40, we treated a subset of mice (ABX mice) continually with broad-spectrum antibiotics (ampicillin and neomycin) to deplete their gut microbiota. One week after initiation of antibiotic treatment, mice were inoculated with tumors and simultaneously treated with three doses of 100 μg αOX40, administered 4 days apart (Figure 2A).

As expected, antibiotic treatment significantly depleted bacterial load in fecal samples collected over the duration of the experiment (Figure S5A). Ten days after αOX40 treatment initiation, serum ALT levels were assessed. At 11 days after treatment initiation, mice were humanely culled and liver NKT cells were assessed by flow cytometry and livers were histologically scored. We found that repeated administration of αOX40 did not lead to elevated levels of ALT in serum (Figure 2B), indicating a lack of αOX40-induced hepatotoxicity. Furthermore, there was no significant difference in αOX40-induced ALT levels in the serum of untreated and antibiotic-treated mice. Assessment of liver tissue by histological scoring revealed significantly increased immune inflammation in the portal and lobular regions of the livers of αOX40-treated mice (Figure 2C–G); however, there were no observable regions of necrosis within the livers of αOX40-treated mice (Figure 2G), indicating that this induction of mild inflammation was insufficient to cause liver damage, or elevate ALT levels in serum. Interestingly, although the induction of liver inflammation did not result in overt toxicity, ABX treatment significantly reduced regions of inflammation after αOX40 treatment, indicating that the gut microbiome does play a key role in mediating immune responses to αOX40 treatment in the liver. We next determined whether liver NKT cells were depleted after repeated dosing of αOX40. Quantification of liver NKT cells after repeated αOX40 dosing showed that these cells were increased, rather than decreased, in both antibiotic-treated and untreated mice following αOX40 treatment. $TCR\beta^+$, $CD4^+$, and $CD8^+$ T cells were also significantly increased after αOX40 treatment (Figure 2H–J). In summary, repeated dosing with αOX40 induced a mild inflammation that is modulated by the gut microbiome but was nonetheless insufficient to induce liver toxicity.

Next, we evaluated the serum cytokine mileu as Lan et al. reported a significant increase in serum cytokines IL-18 and IL-1β as a result of the pyroptosis of liver NKT cells. Consistent with the lack of liver toxicity, serum concentrations of IL-18 and IL-1β were not elevated after αOX40 treatment (Figure 3A,B). However, as reported previously by others,[7,21] αOX40 treatment did induce significantly

FIGURE 2 An alternative αOX40 dosing strategy did not induce hepatotoxicity. (A) Overview of experimental design. (B) Serum concentrations of ALT 10 days post treatment initiation. (C) Representative H&E-stained liver sections 11 days post-treatment initiation. Regions of immune inflammation indicated with arrows. Scale bars are 200 μm in length. Histological liver scoring was used to quantitate (D) total inflammation, (E) portal inflammation, (F) lobular inflammation, and (G) necrosis. Total histological score (D) is the sum of (E–G). (H) Representative flow cytometry gates of liver natural killer T (NKT) cells. Quantification of (I) natural killer T cells (NKT; CD1d-tetramer$^+$TCRβ$^+$), (J) conventional T cells (CD1d-tetramer$^-$TCRβ$^+$), (K) CD4$^+$ TCRβ$^+$ T cells, and (L) CD8$^+$TCRβ$^+$ T cells per gram of liver. A Mann–Whitney test was used to assess statistical significance. *$p \leq 0.05$, **$p \leq 0.01$, ***$p \leq 0.001$, ****$p \leq 0.0001$, n.s. not significant. Data are shown as mean ± SEM (n = 8–10/group)

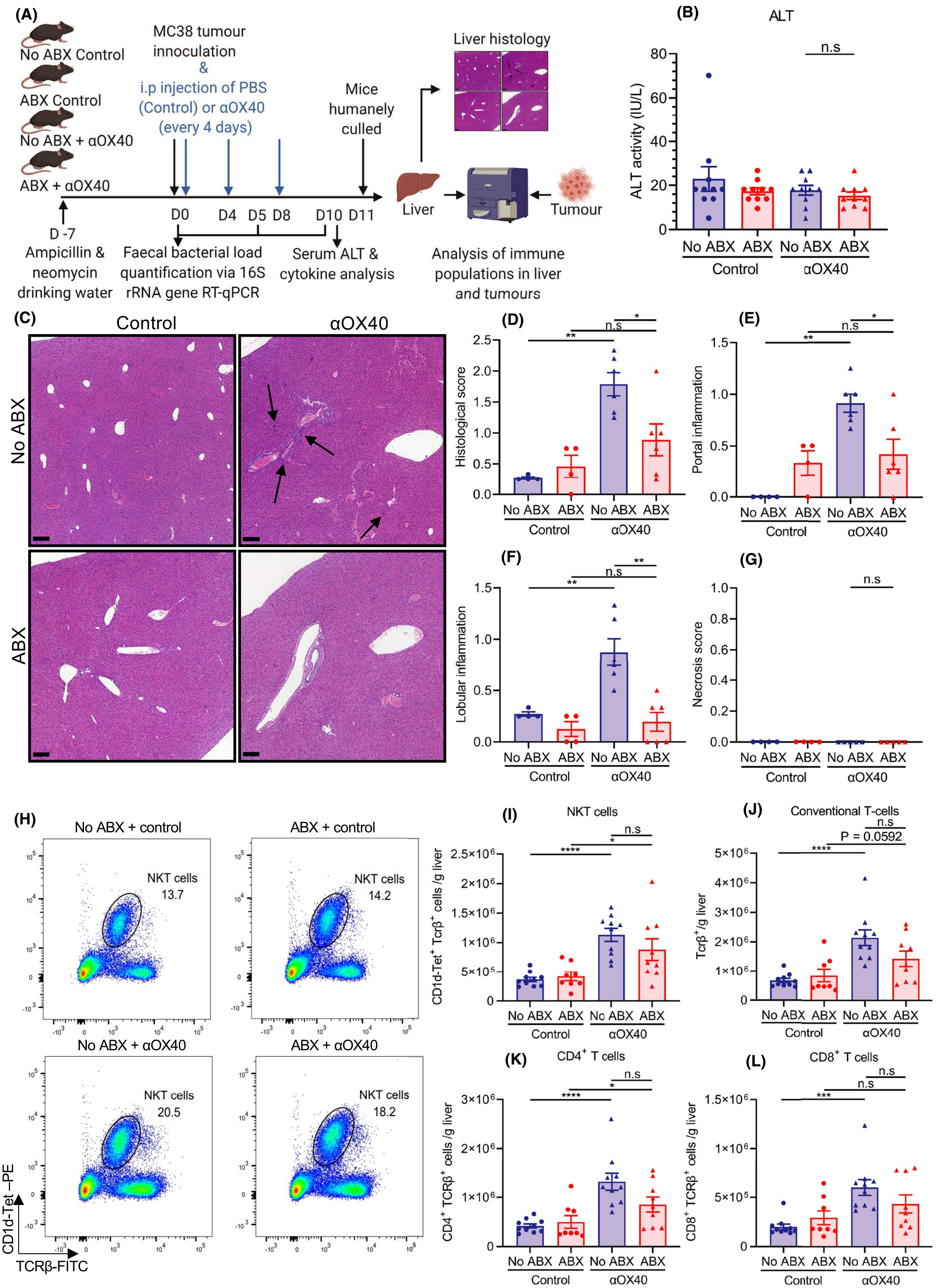
(A)
No ABX Control
ABX Control
No ABX + αOX40
ABX + αOX40
MC38 tumour innoculation
&
i.p injection of PBS (Control) or αOX40 (every 4 days)
Mice humanely culled
Liver histology
Liver
Tumour
D -7
D0
D4
D5
D8
D10
D11
Ampicillin & neomycin drinking water
Faecal bacterial load quantification via 16S rRNA gene RT-qPCR
Serum ALT & cytokine analysis
Analysis of immune populations in liver and tumours
(B)
ALT
ALT activity (IU/L)
n.s
No ABX
ABX
Control
αOX40
(C)
Control
αOX40
No ABX
ABX
(D)
Histological score
(E)
Portal inflammation
(F)
Lobular inflammation
(G)
Necrosis score
(H)
No ABX + control
ABX + control
No ABX + αOX40
ABX + αOX40
NKT cells
13.7
14.2
20.5
18.2
CD1d-Tet –PE
TCRβ-FITC
(I)
NKT cells
CD1d-Tet+ Tcrβ+ cells /g liver
(J)
Conventional T-cells
P = 0.0592
Tcrβ+/g liver
(K)
CD4+ T cells
CD4+ TCRβ+ cells /g liver
(L)
CD8+ T cells
CD8+ TCRβ+ cells /g liver

increased levels of the proinflammatory cytokines TNFα and IL-6 in serum, and significantly reduced levels of the immunosuppressive cytokine, TGFβ, compared to PBS-treated controls (Figure 3C–E). Moreover, αOX40-induced cytokine levels were not significantly different between antibiotic-treated and untreated mice, suggesting that the gut microbiota does not modulate the cytokine release syndrome induced by αOX40.

Due to the lack of αOX40-induced severe hepatotoxicity in our hands, we wanted to confirm that αOX40 was functional as a cancer immunotherapy using this dosing strategy. Consistent with previous reports,[11,15,22] flow cytometry analysis of tumors harvested from control or αOX40-treated mice showed that treatment with αOX40 resulted in a significant increase in tumor-infiltrating $CD8^+$ T cells accompanied by a reduction in tumor Treg cells (Figure 3F–G). These responses in the tumor were not significantly altered by antibiotic treatment. Additionally, to verify that mice in our facility were sensitive to hepatotoxicity driven by liver NKT cells, we treated mice with the mitogen, ConA, which is known to induce acute liver damage driven by lymphocytes, notably NKT cells.[23] As expected, ConA treatment induced severe hepatotoxicity as indicated by highly elevated serum ALT, while also depleting liver NKT cells (Figure S6A–C), indicating the mice used in our experiments are highly sensitive to NKT driven liver damage.

In summary, we found that αOX40 treatment induced significant changes to the tumor T-cell compartment and induced a proinflammatory serum cytokine milieu. However, we were unable to demonstrate that αOX40 treatment led to increased serum IL-1β or IL-18, depleted liver NKT cells, or induced liver necrosis nor elevated ALT levels as was reported by Lan et al.[12] even when given at much higher doses than reported. Given that antibiotic treatment had no significant effect on the majority of these factors, it is unlikely that differences in the gut microbiota between studies explain these different results.

3.3 | Three-week-old mice express higher levels of OX40 but do not experience αOX40 toxicity

We next investigated whether any other possible factors could provide an explanation for this discrepancy with the Lan et al. study.[12] We identified two additional possibilities that could explain the lack of αOX40 toxicity observed in our hands. In our experiments, we had treated MC38 tumor-bearing mice with αOX40, while Lan et al.[12] investigated αOX40 responses in tumor-free mice. Recently, it was shown that subcutaneous inoculation of heterotopic tumor cell lines, including MC38 cells, can alter immune responses systemically,[24] which could therefore potentially alter immune responses to αOX40 and also αOX40-induced toxicity. Another possible factor was the age of mice used. In the study by Lan et al.,[12] some experiments indicated that younger, 3-week-old, mice were used. We evaluated if the expression of OX40 on liver immune cells differed in 3- and 9-week-old mice, which could alter the susceptibility to αOX40-induced toxicity.

We hypothesized that higher expression of OX40 on liver NKT cells in 3-week-old mice may render liver NKT cells in young mice more susceptible to αOX40-induced pyroptosis due to overstimulation of the OX40 pathway. To investigate this, livers from 3- and 9-week-old tumor-free mice were collected and the expression of OX40 on liver immune cells determined. Our data indicate that NKT cells from 3-week-old mice indeed have higher expression of OX40 compared to 9-week-old mice (Figure 4A,B). Increased OX40 expression in younger mice was also observed on NK cells and T cells but not on myeloid $CD11b^+$ cells (Figure 4C–E). However, the majority of analyzed cell populations, including NKT cells did not express high levels of OX40 as indicated by a distinctly stained positive population, contrasting the findings by Lan et al.[12]

Given these findings, we investigated whether younger mice were more susceptible to αOX40-induced liver damage by treating 3-week-old, tumor-free mice with a single 200 μg dose of αOX40, and determining ALT levels and numbers of liver NKT cells 14 days later (Figure 4F). Despite 3-week-old mice expressing higher levels of OX40 on their NKT cells, αOX40 treatment did not induce significantly elevated levels of ALT in serum collected at day 7 or day 14 post-treatment (Figure 4G,H), indicating that αOX40 treatment did not induce significant hepatotoxicity in these mice. Consistent with these data, liver NKT cells were not significantly altered in αOX40-treated mice (Figure 4I,J), indicating that αOX40 did not induce pyroptosis of liver NKT cells in 3-week-old mice. In conclusion, we have investigated responses to αOX40 treatment in a broad range of contexts including assessment of responses by sex, age, different dosing strategies, and in mice depleted of their microbiota and can find no evidence that αOX40 treatment induces significant liver toxicity as has been previously reported.

4 | DISCUSSION

While there are more than 30 ongoing clinical trials investigating the efficacy of αOX40 immunotherapy against a range of different cancers (ClinicalTrials.gov), information regarding the potential toxicity of αOX40 in both preclinical studies and Phase I–II clinical trials is scarce. Significant hepatotoxicity has been reported for many different IAAs in both preclinical and early phase clinical trials,[9,17] which represents a significant roadblock to the clinical use of these

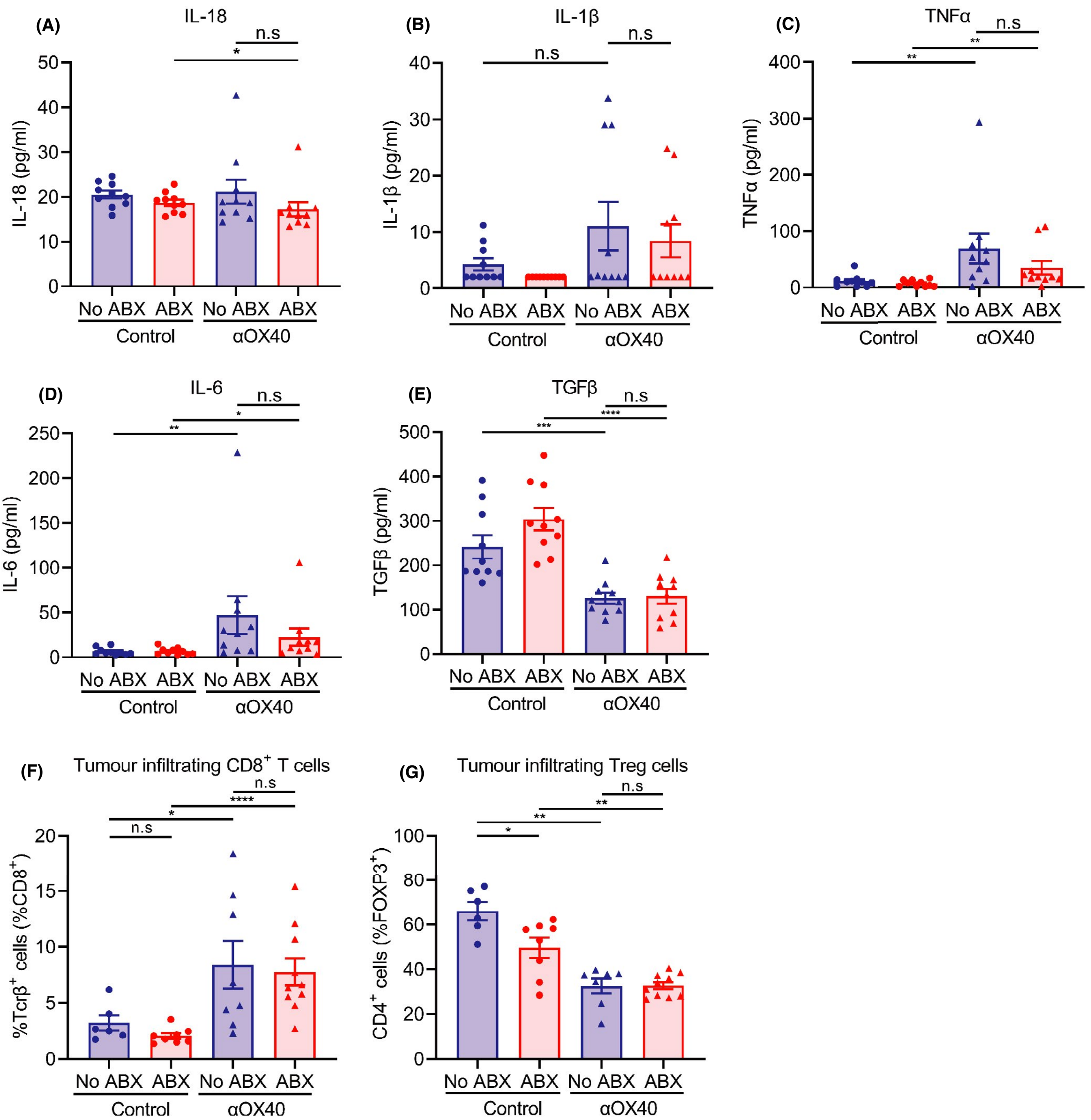

FIGURE 3 αOX40 treatment induces a proinflammatory cytokine milieu without increasing levels of IL-18 and IL-1β in serum. Mice were treated with αOX40 as outlined in (Figure 2A). Serum concentrations of (A) IL-18, (B) IL-1β, (C) TNFα, (D) IL-6, and (E) TGFβ, 10 days post-treatment initiation. MC38 tumor immune infiltration was assessed and the proportion of (F) $TCR\beta^{+}CD8^{+}$ T cells and (G) the proportion of $TCR\beta^{+}CD4^{+}Foxp3^{+}$ regulatory T cells (Treg cells) determined 11 days post-treatment initiation. A Mann–Whitney test was used to assess statistical significance. $*p \leq 0.05$, n.s. not significant. Data are shown as mean ± SEM ($n = 6$–10/group)

immunotherapies. A recent preclinical study has suggested that the IAA, αOX40, induces significant hepatotoxicity in a preclinical model, via the induction of liver NKT cell pyroptosis.[12] Such reports have the potential to dampen the enthusiasm for investigating αOX40 clinically. In contrast to this previous report, we could find no evidence that αOX40 induced significant liver damage in mice, despite extensive investigation of a broad range of factors that could potentially modulate αOX40-induced toxicity including age, sex, dosing strategy, tumor burden, and the gut microbiota.

Prior to the study by Lan et al., the OX40 pathway has been implicated in many autoimmune disorders such as

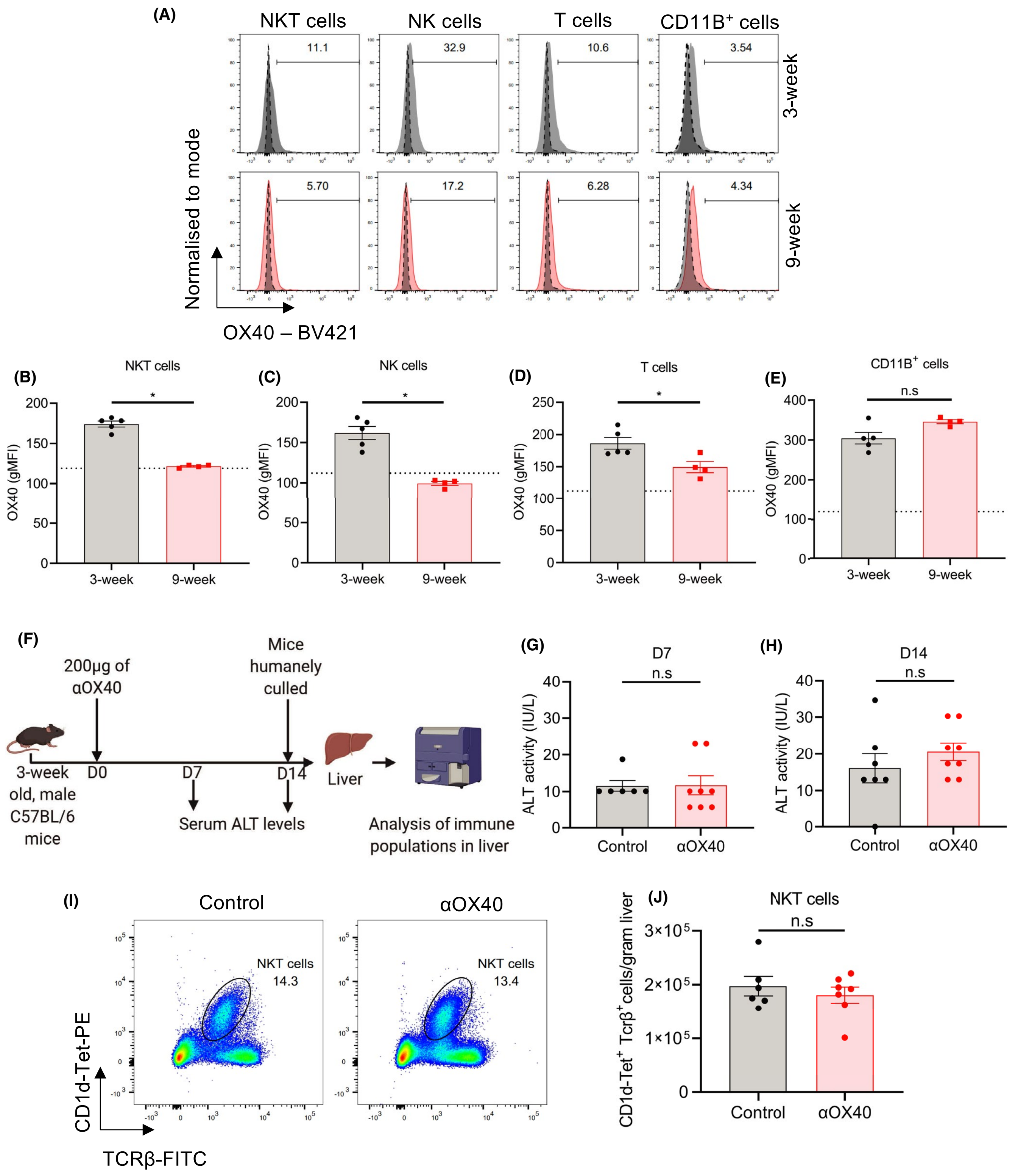

FIGURE 4 3-week-old mice have higher OX40 expression on liver immune cells but not increased hepatotoxicity following αOX40 treatment. (A) Representative histograms of OX40 expression on liver natural killer T (NKT) cells ($CD1d\text{-}Tet^{+}TCR\beta^{+}$), natural killer (NK) cells ($NK1.1^{+}TCR\beta^{-}$), conventional T cells ($NK1.1^{-}TCR\beta^{+}$), and $CD11b^{+}$ myeloid cells ($CD11b^{+}NK1.1^{-}$). Solid plots indicate OX40-stained samples and shaded plots indicate fluorescent minus one (FMO) control without anti-OX40-BV421 antibody. Geometric mean fluorescent intensity (gMFI) of OX40 expression on liver (B) NKT cells, (C) NK cells, (D) T cells, and (E) $CD11b^{+}$ cells from 3-week-old and 9-week-old mice ($n = 4$–5/group). Dotted line indicates gMFI of FMO control. (F) Experimental plan to determine αOX40-induced NKT cell pyroptosis and liver damage in 3-week-old male tumor-free mice ($n = 6$–7/group). Quantification of serum ALT levels at (G) 7 days and (H) 14 days after treatment with αOX40. (I) Representative dot plots of liver NKT cells and (J) number of NKT cells per gram of liver. A Mann–Whitney test was used to assess statistical significance. $^{*}p \leq 0.05$, n.s. not significant. Data are shown as mean ± SEM

colitis, ischemic reperfusion injury, and arthritis[25-28]; however, evidence of liver damage induced by direct stimulation by αOX40 was sparse. Data from three phase I clinical trials of αOX40 suggests that certain αOX40 analogs have the potential to induce mild liver damage in a small proportion of patients as liver damage markers were reported to be mildly elevated (grade 1–2) in 3/28 patients in one of these trials.[29] In this trial, the most severe irAEs were grades 3 and 4 lymphopenia. The second and third trials, using a different αOX40 analog, did not report any evidence of αOX40-induced liver damage.[30,31] These data are consistent with our preclinical data which showed that αOX40 induced very mild liver inflammation, but not the severe liver damage, necrosis, and elevated ALT levels reported by Lan et al.[12]

A potential explanation for the αOX40-induced liver toxicity in the Lan et al. study may be that OX40 expression on liver NKT cells in their study was significantly higher than observed in ours. Liver, spleen, LN, and bone marrow NKT cells in the Lan et al. study expressed OX40 at high levels, while we observed that the majority of liver NKT cells in our mice did not express OX40. Genetic differences are unlikely to explain these differences, as both studies used C57BL/6 mice from Jackson Laboratories as founders for the individual breeding colonies. As OX40 is known to be expressed on lymphocytes following activation, the high OX40 expression on liver NKT cells in the Lan et al. study suggests that these cells were highly activated prior to treatment. This high basal state of activation may prime liver NKT cells into pyroptosis upon excessive αOX40 stimulation, leading to liver injury. Interestingly, Lan et al. did not report increases in OX40 expression on other immune cells in the liver, indicating an NKT cell specific activation. This NKT cell-specific activating effect may be derived through CD1d recognition by NKT cells. $CD1d^+$ NKT cells are known to recognize sphingolipids that are present on certain gut bacterial species such as *Bacteroides fragilis*.[32] Recognition of these sphingolipids has been implicated to generate an anergic state of NKT cells and thus prevent excessive activation. In support of this, mice deficient in *B. fragilis* producing sphingolipids are susceptible to oxazolone-mediated colitis, and the addition of sphingolipids steers NKT cells into an inactivated state, preventing colitis upon this challenge.[33] Whether this effect can also be seen in the liver will require investigation, but due to the close proximity of the liver to the intestine and its constant exposure to gut-derived products via the hepatic portal vein, it is possible that this also occurs in the liver.[34] If the gut microbiota in the mice used in Lan et al. study were deficient in these sphingolipids-producing microbes, it is possible that this resulted in liver NKT cells being more activated. To assess whether the gut microbiota regulates αOX40-induced hepatotoxicity, we treated mice with broad-spectrum antibiotics to deplete their gut (bacterial) microbiota. Antibiotic treatment did not lead to significant NKT cell activation or increased αOX40-induced hepatotoxicity. In fact, the mild liver inflammation induced by αOX40 was reduced in antibiotic-treated mice. These data suggest that differences in the gut microbiota do not explain the discordant observations of αOX40-induced hepatotoxicity in our study and in the Lan et al. study.

Additionally, age and sex as potential factors that may explain the lack of toxicity were also investigated. A study evaluating the efficacy of αOX40 in varying ages of mice found that αOX40 was able to induce a robust antitumor response in 2-month-old but not 12-month-old mice.[35] This fits with our initial hypothesis that younger mice may be more prone to αOX40 activation with may lead them to be more susceptible to αOX40 toxicity. However, treating 3-week-old mice with αOX40, which have higher OX40 expression, we were still unable to observe αOX40-induced toxicity, indicating that differences in the age of the mice used does not explain discordant reports of αOX40-induced toxicity. Furthermore, the sex of the mice did not explain the lack of toxicity as αOX40 did not induce significant hepatotoxicity in either male or female mice.

In conclusion, we could find no evidence to suggest that αOX40 induces significant hepatotoxicity in mice, suggesting that αOX40 is a safer immunotherapy than has been previously suggested warranting further consideration in clinical studies.

ACKNOWLEDGMENTS

We thank the SAHMRI Bioresources facility staff for their assistance with mouse husbandry and breeding. We also acknowledge the SAHMRI flow cytometry core and Randall Grose with his assistance with flow cytometry. We also acknowledge the NIH Tetramer Core Facility for providing the CD1d-Tetramer. Figures with graphical experimental designs were created using BioRender.com.

CONFLICT OF INTEREST

S.J.B. and D.J.L. are co-inventors on International Patent Ap plication No. PCT/AU2020/051278 relating to the effects of the gut microbiota on IAA-induced immunotoxicity. D.J.L. also receives funding from GSK for research not related to this project. All other authors do not declare any competing interests.

AUTHOR CONTRIBUTIONS

Y.C.T., S.J.B., and D.J.L. designed the research; Y.C.T. and S.J.B. performed the research under the direction of D.J.L. All authors wrote and reviewed the manuscript.

ORCID

Yee C. Tee https://orcid.org/0000-0001-9415-960X
Stephen J. Blake https://orcid.org/0000-0002-5954-2993
David J. Lynn https://orcid.org/0000-0003-4664-1404

REFERENCES

1. Sharma P, Allison JP. The future of immune checkpoint therapy. *Science*. 2015;348:56-61.
2. Larkin J, Chiarion-Sileni V, Gonzalez R, et al. Five-year survival with combined nivolumab and ipilimumab in advanced melanoma. *N Engl J Med*. 2019;381:1535-1546.
3. Garon EB, Rizvi NA, Hui R, et al. Pembrolizumab for the treatment of non-small-cell lung cancer. *N Engl J Med*. 2015;372:2018-2028.
4. Duan Q, Zhang H, Zheng J, Zhang L. Turning cold into hot: firing up the tumor microenvironment. *Trends Cancer*. 2020;6:605-618.
5. Mayes PA, Hance KW, Hoos A. The promise and challenges of immune agonist antibody development in cancer. *Nat Rev Drug Discov*. 2018;17:509-527.
6. Guo Z, Wang X, Cheng D, Xia Z, Luan M, Zhang S. PD-1 blockade and OX40 triggering synergistically protects against tumor growth in a murine model of ovarian cancer. *PLoS ONE*. 2014;9:e89350.
7. Messenheimer DJ, Jensen SM, Afentoulis ME, et al. Timing of PD-1 blockade is critical to effective combination immunotherapy with anti-OX40. *Clin Cancer Res*. 2017;23:6165-6177.
8. Suntharalingam G, Perry MR, Ward S, et al. Cytokine storm in a phase 1 trial of the anti-CD28 monoclonal antibody TGN1412. *N Engl J Med*. 2006;355:1018-1028.
9. Vonderheide RH, Flaherty KT, Khalil M, et al. Clinical activity and immune modulation in cancer patients treated with CP-870,893, a novel CD40 agonist monoclonal antibody. *J Clin Oncol*. 2007;25:876-883.
10. Alves Costa Silva C, Facchinetti F, Routy B, Derosa L. New pathways in immune stimulation: targeting OX40. *ESMO Open*. 2020;5:e000573.
11. Peng W, Williams LJ, Xu C, et al. Anti-OX40 antibody directly enhances the function of tumor-reactive CD8+ T cells and synergizes with PI3Kβ inhibition in PTEN loss melanoma. *Clin Cancer Res*. 2019;25:6406-6416.
12. Lan P, Fan Y, Zhao Y, et al. TNF superfamily receptor OX40 triggers invariant NKT cell pyroptosis and liver injury. *J Clin Invest*. 2017;127:2222-2234.
13. Mayer CT, Tian L, Hesse C, et al. Anti-CD4 treatment inhibits autoimmunity in scurfy mice through the attenuation of co-stimulatory signals. *J Autoimmun*. 2014;50:23-32.
14. Nadkarni MA, Martin FE, Jacques NA, Hunter N. Determination of bacterial load by real-time PCR using a broad-range (universal) probe and primers set. *Microbiology*. 2002;148:257-266.
15. Bulliard Y, Jolicoeur R, Zhang J, Dranoff G, Wilson NS, Brogdon JL. OX40 engagement depletes intratumoral Tregs via activating FcgammaRs, leading to antitumor efficacy. *Immunol Cell Biol*. 2014;92:475-480.
16. Bartkowiak T, Jaiswal AR, Ager CR, et al. Activation of 4–1BB on liver myeloid cells triggers hepatitis via an interleukin-27–dependent pathway. *Clin Cancer Res*. 2018;24:1138-1151.
17. Dubrot J, Milheiro F, Alfaro C, et al. Treatment with anti-CD137 mAbs causes intense accumulations of liver T cells without selective antitumor immunotherapeutic effects in this organ. *Cancer Immunol Immunother*. 2010;59:1223-1233.
18. Medina-Echeverz J, Ma C, Duffy AG, et al. Systemic agonistic anti-CD40 treatment of tumor-bearing mice modulates hepatic myeloid-suppressive cells and causes immune-mediated liver damage. *Cancer Immunol Res*. 2015;3:557-566.
19. Ma C, Han M, Heinrich B, et al. Gut microbiome-mediated bile acid metabolism regulates liver cancer via NKT cells. *Science*. 2018;360:eaan5931.
20. Miyake Y, Yamamoto K. Role of gut microbiota in liver diseases. *Hepatol Res*. 2013;43:139-146.
21. So T, Croft M. Cutting edge: OX40 inhibits TGF-β- and antigen-driven conversion of naive CD4 T cells into $CD25^+Foxp3^+$ T cells. *J Immunol*. 2007;179:1427-1430.
22. Piconese S, Valzasina B, Colombo MP. OX40 triggering blocks suppression by regulatory T cells and facilitates tumor rejection. *J Exp Med*. 2008;205:825-839.
23. Heymann F, Hamesch K, Weiskirchen R, Tacke F. The concanavalin A model of acute hepatitis in mice. *Lab Anim*. 2015;49:12-20.
24. Allen BM, Hiam KJ, Burnett CE, et al. Systemic dysfunction and plasticity of the immune macroenvironment in cancer models. *Nat Med*. 2020;26:1125-1134.
25. Jin H, Zhang C, Sun C, et al. OX40 expression in neutrophils promotes hepatic ischemia/reperfusion injury. *JCI Insight*. 2019;4.
26. Murata K, Nose M, Ndhlovu LC, Sato T, Sugamura K, Ishii N. Constitutive OX40/OX40 ligand interaction induces autoimmune-like diseases. *J Immunol*. 2002;169:4628-4636.
27. Stuber E, Buschenfeld A, Luttges J, Von Freier A, Arendt T, Folsch UR. The expression of OX40 in immunologically mediated diseases of the gastrointestinal tract (celiac disease, Crohn's disease, ulcerative colitis). *Eur J Clin Invest*. 2000;30:594-599.
28. Giacomelli R, Passacantando A, Perricone R, et al. T lymphocytes in the synovial fluid of patients with active rheumatoid arthritis display CD134-OX40 surface antigen. *Clin Exp Rheumatol*. 2001;19:317-320.
29. Curti BD, Kovacsovics-Bankowski M, Morris N, et al. OX40 is a potent immune-stimulating target in late-stage cancer patients. *Cancer Res*. 2013;73:7189-7198.
30. El-Khoueiry AB, Hamid O, Thompson JA, et al. The relationship of pharmacodynamics (PD) and pharmacokinetics (PK) to clinical outcomes in a phase I study of OX40 agonistic monoclonal antibody (mAb) PF-04518600 (PF-8600). *J Clin Oncol*. 2017;35:3027.
31. Glisson BS, Leidner RS, Ferris RL, et al. Safety and clinical activity of MEDI0562, a humanized OX40 agonist monoclonal antibody, in adult patients with advanced solid tumors. *Clin Cancer Res*. 2020;26:5358-5367.
32. Brown EM, Ke X, Hitchcock D, et al. Bacteroides-derived sphingolipids are critical for maintaining intestinal homeostasis and symbiosis. *Cell Host Microbe*. 2019;25:668-680.e7.
33. An D, Oh SF, Olszak T, et al. Sphingolipids from a symbiotic microbe regulate homeostasis of host intestinal natural killer T cells. *Cell*. 2014;156:123-133.
34. Tripathi A, Debelius J, Brenner DA, et al. The gut-liver axis and the intersection with the microbiome. *Nat Rev Gastroenterol Hepatol*. 2018;15:397-411.
35. Ruby CE, Weinberg AD. OX40-enhanced tumor rejection and effector T cell differentiation decreases with age. *J Immunol*. 2009;182:1481-1489.

SUPPORTING INFORMATION

Additional supporting information may be found online in the Supporting Information section.

How to cite this article: Tee YC, Blake SJ, Lynn DJ. OX40-targeted immune agonist antibodies induce potent antitumor immune responses without inducing liver damage in mice. *FASEB BioAdvances*. 2021;3:829–840. https://doi.org/10.1096/fba.2021-00039